ISIJ International, Vol. 44 (2004), No. 10, pp. 1623–1628

Occurrence Condition for a Swirl Motion of a Bath Agitated by Bottom Gas Injection

Manabu IGUCHI, Daisuke IGUCHI,[1] Yasushi SASAKI,[2] Takehiko KUMAGAI and Shinichiro YOKOYA[3]

Division of Materials Science and Engineering, Graduate School of Engineering, Hokkaido University, North 13, West 8, Kita-ku, Sapporo 060-8628 Japan. 1) Visiting Researcher, Graduate School of Engineering, Hokkaido University, North 13, West 8, Kita-ku, Sapporo 060-8628 Japan. 2) Department of Metallurgy, Graduate School of Engineering, Tohoku University, 2 Aza-aoba, Aramaki, Sendai, Miyagi 980-8579 Japan. 3) Department of Mechanical Engineering, Nippon Institute of Technology, Miyashiro, Minami-Saitama, Saitama 345-8501 Japan.

(*Received on April 12, 2004; accepted in final form on July 26, 2004*)

A swirl motion of a cylindrical bath appears under a certain condition when the bath is agitated by bottom gas injection. The swirl motion can be classified into two types. One is called the shallow-water wave type, and the other is called the deep-water wave type. The condition for the occurrence of a swirl motion of the deep-water wave type was experimentally investigated based on water model experiments. Empirical equations were proposed for predicting the condition as functions of the gas flow rate, vessel diameter, inner diameter of the nozzle, and the physical properties of fluids.

KEY WORDS: steelmaking; refining; swirl motion; wastewater treatment; bubbling jet; injection.

1. Introduction

A swirl motion of a cylindrical bath agitated by bottom gas injection occurs under a certain blowing condition due to a hydrodynamic instability.[1–7] There appear two types of swirl motions depending on the aspect ratio of the bath, A_s ($=H_L/D$), as schematically shown in **Fig. 1**, where H_L is the bath depth and D is the vessel diameter. One is called the shallow-water wave type and the other is called the deep-water wave type.[2] The boundary between the two types of swirl motions is located around an aspect ratio of the bath, H_L/D, of 0.3. The shallow-water wave type is affected by the bottom wall as well as the side wall of the vessel. On the other hand, the deep-water wave type is affected only by the side wall of the vessel. Accordingly, the liquid in a bath of H_L/D greater than about 0.3 is much more easier to move than that in a bath of H_L/D smaller than about 0.3. The two types of swirl motions are very similar to rotary sloshing[8,9] caused by oscillating a cylindrical bath in the horizontal or vertical direction.

The characteristics of the swirl motions have been investigated by many researchers, and, as a result, much information is available.[1–7] For example, the periods of the two swirl motions were satisfactorily predicted by the periods of the rotary sloshing of the shallow-water and deep-water wave types, respectively. The occurrence condition for the swirl motion, however, is not fully understood yet.

A swirl motion of the deep-water wave type is of practical importance in steelmaking as well as wastewater treatment.[10,11] In this study particular attention was paid to the occurrence condition for the swirl motion of the deep-water wave type. Some empirical equations were proposed for predicting the condition.

2. Experiment

Figure 2 shows a schematic of the experimental apparatus for water model experiments. The cylindrical test vessel was made of transparent acrylic resin. Water and air were used as the working fluids. Air was injected through a centered single-hole nozzle. The vessel diameter, D, was varied from 80 to 390 mm. The inner diameter of the nozzle, d_{ni}, was 1.0, 1.5, 2.0, 4.0, and 5.0 mm. The test vessel was enclosed with another vessel with a rectangular cross-section made of the same transparent acrylic resin. The clearance

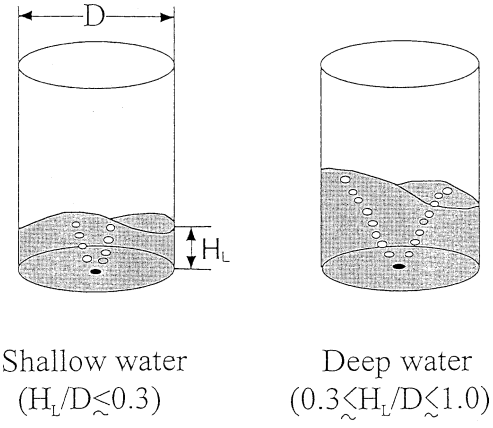

Fig. 1. Classification of swirl motions of a bath agitated by bottom gas injection.

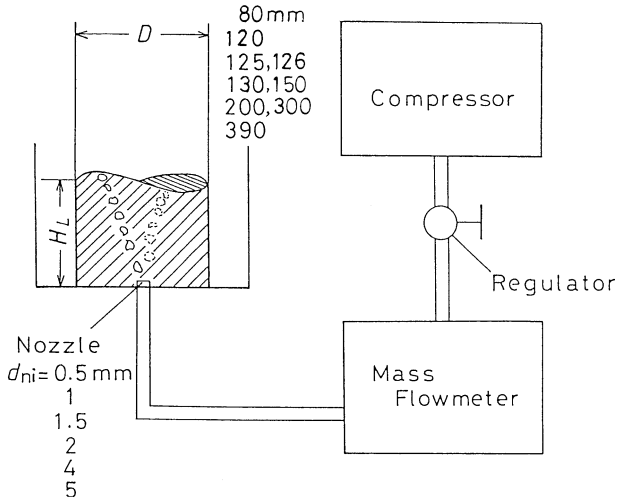

Fig. 2. Experimental apparatus.

between the rectangular vessel and the cylindrical vessel was filled with water to avoid distortion of video images of a swirl motion of the bath. Occurrence of a swirl motion of the deep-water wave type was judged with a digital video camera and by eye inspection. The measurements were repeated more than two times under every experimental condition to determine the critical condition for the occurrence of the swirl motion.

3. Prediction of Occurrence Conditions of Swirl Motion

In a previous paper,[12] the authors proposed some methods for predicting the occurrence condition of a swirl motion of a bath agitated by a bottom blown liquid jet. The mechanism of the occurrence of the swirl motion of a bath agitated by bottom gas injection seems to resemble that of a bath agitated by a bottom blown liquid jet. Firstly, a brief explanation will be given on the previously proposed prediction methods for a bath agitated by a bottom blown liquid jet.[12] Secondly, some prediction methods will be proposed for a bath agitated by bottom gas injection.

3.1 Preferable Occurrence Condition for Swirl Motion of a Bath Agitated by Bottom Blown Liquid Jet

The boundary of the region in which a cylindrical bath agitated by a bottom blown liquid jet exhibits a swirl motion can be correlated in terms of the aspect ratio, H_L/D, and the following modified Rossby number,[13] Ro_m.

$$Ro_m = Q_L^2/(g d_{nen}^2 D^3) \quad \text{.....(1)}$$

where Q_L is the liquid flow rate, g is the acceleration due to gravity, d_{nen} is the inner nozzle diameter, and D is the vessel diameter. This dimensionless number represents a ratio of the inertial force of the injected liquid to the centrifugal force acting on the liquid in the bath. **Figure 3** shows an example of the occurrence region of the swirl motion as a function of the aspect ratio, H_L/D, and the modified Rossby number, Ro_m. The boundary is divided into four sub-boundaries, (1), (2), (3), and (4). A prediction method was given on each sub-boundary in the previous paper.[12] The same methods will be applied to predicting the boundary of the occurrence region of a swirl motion of a bath agitated by

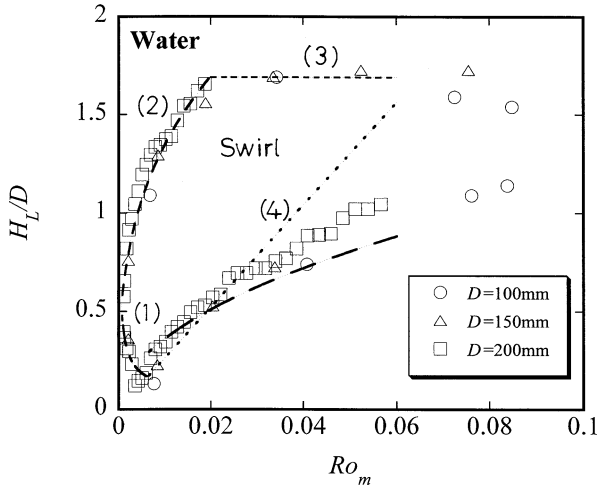

Fig. 3. Occurrence region of swirl motion in a bath agitated by bottom liquid injection.

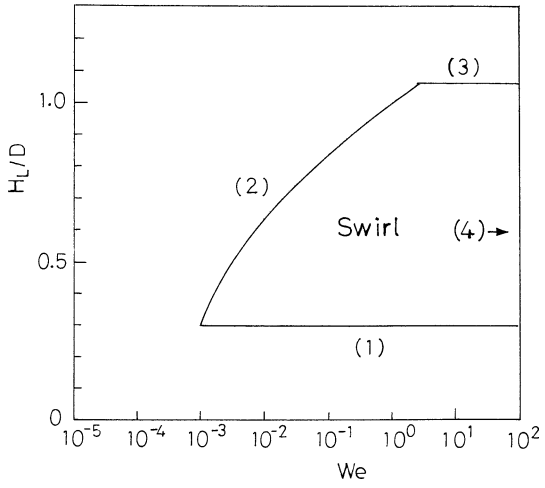

Fig. 4. Schematic of swirl motion appearing in a bath agitated by bottom gas injection.

bottom gas injection.

3.2. Preferable Occurrence Condition for Swirl Motion of a Bath Agitated by Bottom Gas Injection

According to the previous water model experiments,[2] the boundary of the region in which a bath agitated by a bottom gas injection exhibits a swirl motion can be correlated in terms of the aspect ratio, H_L/D, and the following modified Weber number, We.

$$We = \rho_L Q_g^2/(\sigma D^3) \quad \text{.....(2)}$$

where ρ_L is the density of liquid, Q_g is the gas flow rate, σ is the surface tension. This dimensionless number represents a ratio of the inertial force of bubbling jet to the surface tension force acting on the meniscus. The boundary of the occurrence region can be schematically shown in **Fig. 4**. The boundary also seems to be divided into four sub-boundaries, although the sub-boundary (4) cannot be clearly identified at present. Discussion will be given on each sub-boundary in the next section.

3.3. Prediction of Four Sub-boundaries

3.3.1. Sub-boundary (1)

According to the previous paper[12] for a bath agitated by

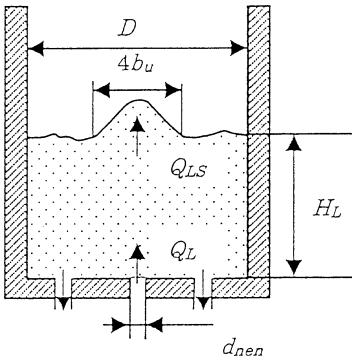

Fig. 5. Elevated surface of a bath agitated by bottom liquid injection.

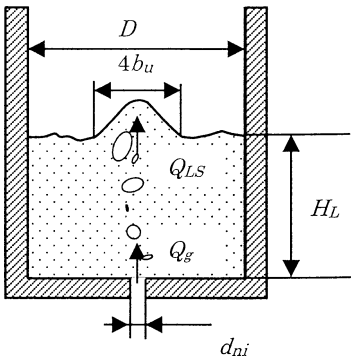

Fig. 6. Elevated surface of a bath agitated by bottom gas injection.

a liquid jet (see **Fig. 5**), a swirl motion around the sub-boundary (1) occurs when an imaginary height of the elevated bath surface, H_{LeB}, caused by impingement of the liquid jet exceeds a certain critical value. This condition can be expressed for a bath agitated by bottom gas injection (see **Fig. 6**):

$$H_{LeB}/D \geq k_1' \quad \text{.....(3)}$$

$$H_{LeB}=[Q_{Ls}/(\pi D^2/4)]^2/(2g) \quad \text{.....(4)}$$

$$Q_{Ls}=3.6u_{L,cl}b_u^2 \quad \text{.....(5)}$$

$$u_{L,cl}=k_{12}(g^2Q_g)^{1/5} \quad \text{.....(6)}$$

$$b_u=0.14H_L \quad \text{.....(7)}$$

where k_1' and k_{12} are constants, Q_{Ls} is the liquid flow rate at the bath surface,[12,14–17] $u_{L,cl}$ is the centerline velocity of liquid flow, b_u is the half-value radius of the axial velocity distribution of the liquid flow, and H_L is the bath depth. The bubble dispersion region in the bath is called the bubbling jet. The liquid flow was induced mainly by the buoyancy force acting on bubbles in the bubbling jet. In Eq. (4) $Q_{Ls}/(\pi D^2/4)$ means an imaginary cross-sectional mean velocity induced by the bubbling jet on the bath surface.

Substitution of Eqs. (4) through (7) into Eq. (3) yields

$$H_L/D \geq k_1 Fr_{mD}^{-1/20} \quad \text{.....(8)}$$

$$Fr_{mD}=Q_g^2/(gD^5) \quad \text{.....(9)}$$

where Fr_{mD} is a modified Froude number. The coefficient, k_1, can be determined by fitting Eq. (8) to the existing measured values for the sub-boundary (1) to give

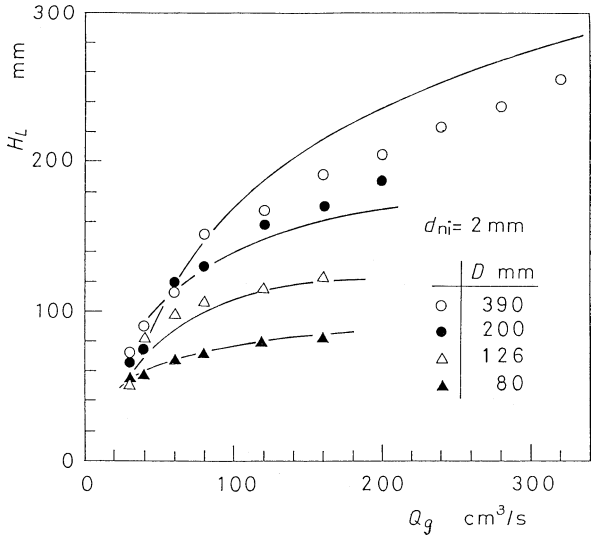

Fig. 7. Critical bath depth for sub-boundary (2) in a bath agitated by bottom gas injection (water–air system, solid line: Eq. (18)).

$$k_1=0.19 \quad \text{.....(10)}$$

Accordingly, the sub-boundary (1) is expressed by

$$H_L/D=0.19Fr_{mD}^{-1/20} \quad \text{.....(11)}$$

Under the present experimental conditions, Eq. (11) gives H_L/D of approximately 0.3 which corresponds to the boundary between the shallow and deep baths. The validity of Eq. (11) will be demonstrated in a later section.

3.3.2. Sub-boundary (2)

(1) Concerning a bath agitated by a bottom blown liquid jet, a swirl motion appears when the pressure fluctuation at the bath surface exceeds a certain critical value.[12] The same criterion is chosen for a bath agitated by bottom gas injection.

$$\rho_L g[Q_{Ls}/(4\pi b_u^2)]^2/(2g)/(\rho_L g H_L) \geq k_2' \quad \text{.....(12)}$$

where k_2' is a constant and $\rho_L g H_L$ is the initial static pressure on the bottom wall of the vessel. In Eq. (12) $[Q_{Ls}/(4\pi b_u^2)]^2/(2g)$ indicates the mean height of the elevated bath surface.

Substitution of Eqs. (5) and (7) into Eq. (12) gives

$$H_L/D \leq k_2 Fr_{mD}^{1/5} \quad \text{.....(13)}$$

The sub-boundary (3) is expressed by

$$H_L/D=k_2 Fr_{mD}^{1/5} \quad \text{.....(14)}$$

Equation (14) reduces to

$$H_L=k_2(Q_g^2/g)^{1/5} \quad \text{.....(15)}$$

This equation states that the critical bath depth is not dependent on the vessel diameter, D. However, the critical bath depth is actually dependent on D, and hence, Eq. (14) is not adequate, as suggested from **Fig. 7**. The measured values are reproduced from the previous paper.[2] The solid lines denote calculated values from Eq. (18) shown below.

(2) Correlation based on modified Weber number: In the previous paper[2] we proposed the following empirical equation for the sub-boundary (2) for a bath agitated by bottom gas injection.

$$\log(H_L/D)=0.05-1.35(X+6)/[\exp(X+5)] \quad \text{.....(16)}$$

$$X=\log We \quad \text{.....(17)}$$

This equation is known to be a good approximation for the sub-boundary (2). However, it is rather complicated, and accordingly, the following equation is newly derived.

$$H_L/D=(1+0.3X)^{1/2} \quad \text{.....(18)}$$

Equation (18) can approximate Eq. (16) within deviation of ±5%.

3.3.3. Sub-boundary (3)

A prediction method for the sub-boundary (3) will be rewritten in the following for a better understanding of this sub-boundary. We assume that the swirl motion ceases when the diameter of the jet on the bath surface, D_{jet}, exceeds a certain critical value (see Fig. 5).[12,18]

$$D_{jet}/D>k_3' \quad \text{.....(19)}$$

where k_3' is a constant. The diameter of the jet, D_{jet}, is defined as

$$D_{jet}=4b_u \quad \text{.....(20)}$$

where b_u is the half-value radius expressed by Eq. (7). The previous study[15] revealed that the sub-boundary (3) is expressed by

$$D_{jet}/D=0.61 \quad \text{.....(21)}$$

If Eq. (21) is valid in the present case, the sub-boundary (3) is expressed by

$$H_L/D=1.06 \quad \text{.....(22)}$$

3.3.4. Sub-boundary (4)

By referring to the discussion on the sub-boundary (4) in a bath agitated by bottom liquid injection,[12] the following first two methods will be proposed for a bath agitated by bottom gas injection.

(1) A swirl motion is assumed to cease when the inertial force of the injected gas, F_i, becomes greater than a certain critical value.

$$F_i/W_{LB}>k_{41}' \quad \text{.....(23)}$$

$$F_i=\rho_g Q_g^2/(\pi d_{ni}^2/4) \quad \text{.....(24)}$$

$$W_{LB}=\rho_L g H_L \pi D^2/4 \quad \text{.....(25)}$$

where W_{LB} is the weight of the liquid in the bath and k_{41}' is a constant. Substitution of Eqs. (24) and (25) into Eq. (23) yields

$$H_L/D<k_{41}\rho_g Q_g^2/(\rho_L g d_{ni}^2 D^3) \quad \text{.....(26)}$$

where k_{41} is a constant. The sub-boundary (4) is expressed by

$$H_L/D=k_{41}\rho_g Q_g^2/(\rho_L g d_{ni}^2 D^3) \quad \text{.....(27)}$$

This equation is not valid, although the evidence is not shown in this paper.

(2) We assume that the swirl motion ceases when the height of the locally elevated interface exceeds a certain critical value.[12]

$$[Q_{Ls}/(4\pi b_u^2)]^2/(2g)/D\geq k_{42}' \quad \text{.....(28)}$$

where k_{42}' is a constant. Equation (28) reduces to

$$Q_g^2/(gD^5)\geq k_{42} \quad \text{..... (29)}$$

The sub-boundary (4) is expressed by

$$Q_g^2/(gD^5)=k_{42} \quad \text{.....(30)}$$

where k_{42} is a constant. This equation also was not adequate. Therefore, we will propose another type of prediction method in the following.

(3) Correlation based on the penetration depth of injected gas: For top and side gas injection through a lance the penetration depth in the bath is expressed as a function of the inner nozzle diameter, d_{ni}, and another type of modified Froude number,[19,20] Fr_m.

$$Fr_m=\rho_g Q_g^2/(\rho_L g d_{ni}^5) \quad \text{.....(31)}$$

The penetration depth is a measure of the position to which an effect of the inertial force of injected gas reaches. Concerning a bottom blown bubbling jet, the penetration depth is not clearly identified but the following length scale is used to show the region in which the inertial force of injected gas plays an essential role.[21,22]

$$z_0=5.0 d_{ni} Fr_m^{0.30} \quad \text{.....(32)}$$

where z_0 is the axial position at which gas holdup is 50%. We assume that a swirl motion ceases when the following condition is satisfied.

$$z_0/H_L>k_{43}' \quad \text{..... (33)}$$

where k_{43}' is a constant. This relationship states that the sub-boundary (4) is expressed by

$$H_L/D=k_{43}[\rho_g Q_g^2/(\rho_L g)]^{0.30}/(D d_{ni}^{0.5}) \quad \text{.....(34)}$$

where k_{43} is a constant. The adequacy of Eq. (34) will be shown later.

4. Experimental Results and Discussion

4.1. Sub-boundary (1)

Some experimental results on the sub-boundary (1) are available in literature. The present authors previously reported that the sub-boundary (1) is given by

$$H_L/D=0.3 \quad \text{.....(35)}$$

This value of 0.3 agrees with the boundary between the shallow and deep baths.[8,9] Figures 8 and 9 demonstrate that the sub-boundary (1) appears to be more precisely predicted by Eq. (11) than Eq. (35).

4.2. Sub-boundary (2)

The adequacy of Eq. (16) for the sub-boundary (2) was already confirmed.[2] Accordingly, only Eq. (18) was compared with the measured values in Figs. 7 through 9. Equation (18) can satisfactorily approximate the measured values.

4.3. Sub-boundary (3)

The sub-boundary (3) appears at a gas flow rate much higher than the maximum gas flow rate shown in **Figs. 8** and **9**. Further information is available in the previous paper.[15]

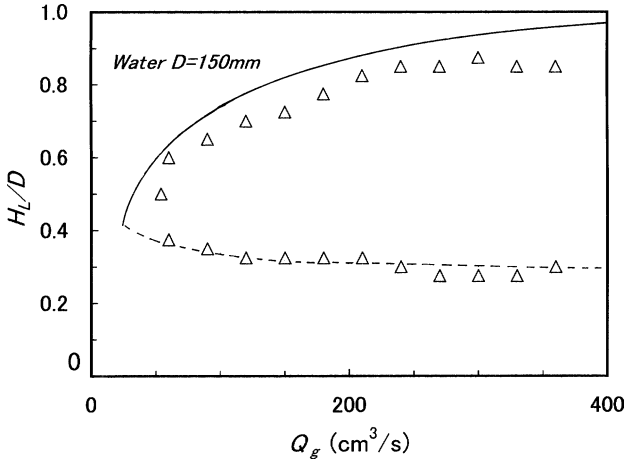

Fig. 8. Comparison of predicted with measured values showing the sub-boundaries (1) and (2) for D=150 mm and d_{ni}=2 mm (broken line: Eq. (11), solid line: Eq. (18)).

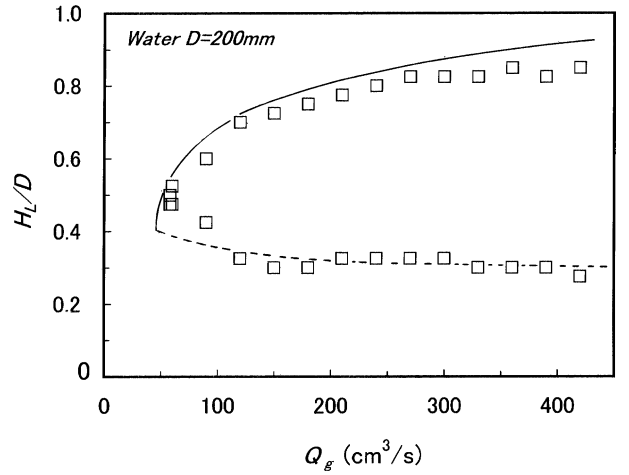

Fig. 9. Comparison of predicted with measured values showing the sub-boundaries (1) and (2) for D=200 mm and d_{ni}=2 mm (broken line: Eq. (11), solid line: Eq. (18)).

4.4. Sub-boundary (4)

The aspect ratio showing the sub-boundary (4) was measured for vessels of D=120 mm and 200 mm. The measured values of the critical aspect ratio are shown against gas flow rate in **Fig. 10**. The sub-boundary (4) is dependent on the gas flow rate, Q_g, inner diameter of the nozzle, d_{ni}, and the inner diameter of the vessel, D. **Figure 11** shows that the measured values of H_L/D are satisfactorily correlated with $[\rho_g Q_g^2/(\rho_L g)]^{0.30}/(Dd_{ni}^{0.5})$. Accordingly, the following empirical equation was derived.

$$H_L/D=3.4[\rho_g Q_g^2/(\rho_L g)]^{0.30}/(Dd_{ni}^{0.5}) \quad .....(36)$$

5. Conclusions

The critical condition for the occurrence of a swirl motion of the deep-water wave type in a bath agitated by bottom gas injection was experimentally investigated. The boundary of the preferable occurrence region of the swirl motion was divided into four sub-boundaries. The following empirical equations were proposed.

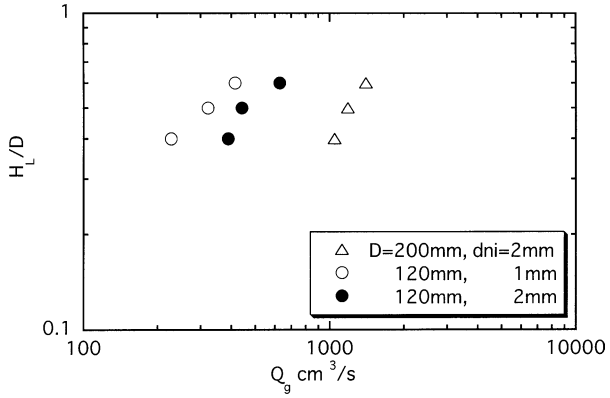

Fig. 10. Critical bath depth for sub-boundary (4) in a bath agitated by bottom gas injection.

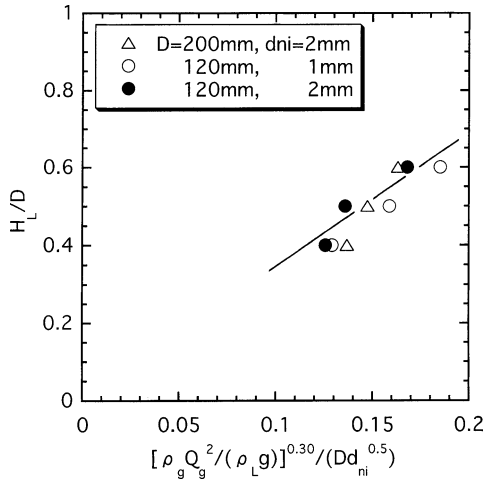

Fig. 11. Correlation of sub-boundary (4) in a bath agitated by bottom gas injection (solid line: Eq. (36)).

(1) Sub-boundary (1)

$$H_L/D=0.19\,Fr_{mD}^{-1/20} \quad .....(11)$$

(2) Sub-boundary (2)

$$H_L/D=(1+0.3\log We)^{1/2} \quad .....(18)$$

(3) Sub-boundary (3)

$$H_L/D=1.06 \quad .....(22)$$

(4) Sub-boundary (4)

$$H_L/D=3.4[\rho_g Q_g^2/(\rho_L g)]^{0.30}/(Dd_{ni}^{0.5}) \quad .....(36)$$

Nomenclature

A_s: Aspect ratio (−)
b_u: Half-value radius of liquid jet (mm)
D: Vessel diameter (mm)
D_{jet}: Diameter of jet on the bath surface (mm)
d_{ni}, d_{nen}: Inner nozzle diameter (mm)
F_i: Inertial force of injected gas (N)
g: Gravitational acceleration (cm/s^2)
H_L: Bath depth (mm)
H_{LeB}: Height of elevated bath surface (mm)
Q_g: Injected gas flow rate (cm^3/s)
Q_L: Injected liquid flow rate (cm^3/s)
Q_{Ls}: Liquid flow rate on the bath surface (cm^3/s)
Ro_m: Modified Rossby number (−)

We: Modified Weber number (−)
W_{LB}: Weight of liquid in bath (N)
ρ_g: Density of gas (kg/m^3)
ρ_L: Density of liquid (kg/m^3)

REFERENCES

1) Y. Kato, K. Nakanishi, T. Nozaki, K. Suzuki and T. Emi: *Tetsu-to-Hagané*, **68** (1982), 1604.
2) M. Iguchi, S. Hosohara, T. Koga, R. Yamaguchi and Z. Morita: *ISIJ Int.*, **33** (1993), 1037.
3) Y. Xie and F. Oeters: *Steel Res.*, **63** (1992), 227.
4) M. P. Schwartz: *Chem. Eng. Sci.*, **45** (1990), 1765.
5) M. Iguchi, Y. Itoh and Z. Morita: *Tetsu-to-Hagané*, **80** (1994), 189.
6) G. G. K. Murthy, S. P. Mehrorta and A. Ghosh: *Metall. Trans. B*, **19** (1988), 839.
7) M. Iguchi, Y. Eguchi, A. Kawasaki, S. Kitamura and K. Naito: *ISIJ Int.*, **39** (1999), 767.
8) A. Kimura and H. Ohashi: *Trans. Jpn. Soc. Mech. Eng.*, **44** (1978), 3024.
9) A. Kimura and H. Ohashi: *Trans. Jpn. Soc. Mech. Eng.*, **44** (1978), 3446.
10) M. Shitara, M. Iguchi, K. Takano, T. Tamamori, H. Shitara and T. Maruyama: *Mater. Trans.*, **44** (2003), No. 12, 2656.
11) M. Shitara, M. Iguchi and T. Tamamori: Proc. 7th Organized Multiphase Flow Forum (Multiphase Flow and Recyle-oriented Technology), (2003), 35.
12) M. Iguchi, D. Iguchi and J. Yoshida: *Mater. Trans.*, **45** (2004), No. 5, 1764.
13) J, Yoshida, D. Iguchi, M. Shitara and M. Iguchi: *ISIJ Int.*, **43** (2003), No. 12, 1890.
14) D. Iguchi, J. Yoshida and M. Iguchi: *Tetsu-to-Hagané*, **90** (2004), No. 6, 357.
15) M. Iguchi, H. Takeuchi and Z. Morita: *ISIJ Int.*, **31** (1991), No. 3, 246.
16) M. Iguchi, J. Tani, T. Uemura, H. Kawabata, H. Takeuchi and Z. Morita: *ISIJ Int.*, **29** (1989), No. 4, 309.
17) M. Iguchi, K. Okita, T. Nakatani and N. Kasai: *Int. J. Multiphase Flow*, **23** (1997), No. 2, 249.
18) M. Shitara, M. Iguchi, T. Tamamori, J. Yoshida and D. Iguchi: *Tetsu-to-Hagané*, **90** (2004), No. 6, 345.
19) B. U. N. Igwe, S. Ramachandran and J. C. Fulton: *Metall. Trans.*, **4** (1973), 1887.
20) M. Iguchi, S. Kodani and H. Tokunaga: *Steel Res.*, **71** (2000), No. 11, 435.
21) T. H. Tacke, H. G. Schubert, D. J. Weber and K. Schwerdtfeger: *Metall. Trans. B*, **16B** (1985), 263.
22) M. Iguchi, K. Nozawa and Z. Morita: *ISIJ Int.*, **31** (1991), No. 9, 952.